Atmospheric Environment 268 (2022) 118763

Contents lists available at ScienceDirect

Atmospheric Environment

journal homepage: www.elsevier.com/locate/atmosenv

Methane emissions in Kuwait: Plume identification, isotopic characterisation and inventory verification

A. Al-Shalan [a,*], D. Lowry [a], R.E. Fisher [a], E.G. Nisbet [a], G. Zazzeri [b], M. Al-Sarawi [c], J.L. France [a,d]

[a] Dept. of Earth Sciences, Royal Holloway, Univ. of London, Egham, TW20 0EX, UK
[b] Dept. of Physics, Imperial College London, South Kensington, London, SW7 2BW, UK
[c] Dept. of Earth and Environmental Sciences, College of Science, Kuwait University, P.O. Box:5969, Safat, 13060, Kuwait
[d] British Antarctic Survey, High Cross, Madingley Rd, Cambridge, CB3 0ET, UK

HIGHLIGHTS

- Weekly sampling and methane isotopic analysis for 3 Kuwait sites over 2 years.
- Mobile CH_4 measurement campaign for 7 days with subsequent GIS mapping.
- Characterization of methane sources into fossil fuel, waste and ruminant categories.
- Diurnal sampling in Kuwait City suburb identifies landfill as main methane source.
- Isotopes identify waste as main source, not fossil fuels as in EDGAR inventory.

GRAPHICAL ABSTRACT

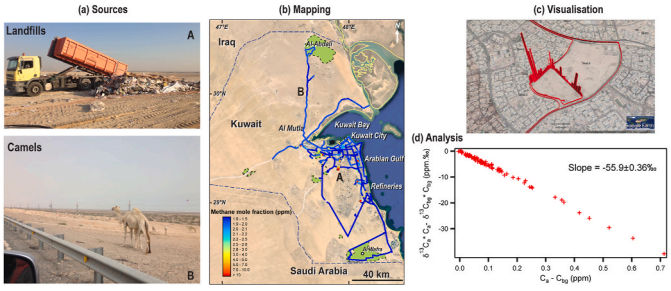

ARTICLE INFO

Keywords:
Plume mapping
Carbon isotopes
Landfill sites
Emissions inventory

ABSTRACT

The distribution of methane sources in Kuwait was mapped through mobile vehicle surveying of methane mole fraction, and by collection of air samples at source for subsequent isotopic analysis. Mobile plume identification and isotopic analysis, reveals that by far the largest observed source of methane in Kuwait is from landfill sites ($\delta^{13}C_{CH4}$ of −58‰), with smaller contributions from fossil fuel industry (−50‰), wastewater treatment (−49‰) and ruminant animals (sheep −64‰, cows, −62‰, camels −60‰).

Regular weekly air samples were collected over two years from three sites in Kuwait, one NW of the city, one to the SE and one in the city from the rooftop of the Kuwait College of Science. Associated with higher mole fraction is a consistent depletion in ^{13}C of methane, pointing to a national source mix with $\delta^{13}C_{CH4}$ of −55.9‰. This is significantly different from calculations using EDGAR v.5 inventory that suggest a source mix of −52.8‰. Diurnal campaigns from a city location confirm that the sources are dominantly biogenic (−59 to −56‰) in and around the urban areas.

The EDGAR 5.0 inventory suggests that the dominant sources of methane in Kuwait are leaks from gas flaring and fossil fuel distribution, with additional smaller emissions from landfills, sewage (wastewater) treatment and ruminant animals, but with a waste component increasing relative to fossil fuel emissions in recent decades. Measurements during 2015 and 2016 suggest that for all but the far south and SW of the country which is not in the meteorological footprint of fixed site or mobile measurement, there is a dominant waste source and much smaller observed proportion from fossil fuel activities.

* Corresponding author.
E-mail address: Aliah.Alshalan.2014@live.rhul.ac.uk (A. Al-Shalan).

https://doi.org/10.1016/j.atmosenv.2021.118763
Received 8 December 2020; Received in revised form 13 September 2021; Accepted 26 September 2021
Available online 29 September 2021

This research demonstrates for the first time in Kuwait that continuous mobile measurements for plume identification coupled with high-precision isotopic analysis using CF-GC-IRMS (Continuous Flow Gas Chromatography-Isotope Ratio Mass Spectrometry) is an effective way of identifying methane sources and understanding their relative contributions. To unambiguously quantify relative contributions will require further work, particularly in the SW region of the country, utilizing aircraft and/or satellite retrievals. The results of this research will contribute to understanding the methane budget of this poorly studied region.

1. Introduction

Atmospheric methane (CH_4) is the second most important anthropogenic greenhouse gas contributing to climate change after CO_2 (Wuebbles and Hayhoe, 2002; Saunois et al. 2016). The atmospheric methane mole fraction is now nearly three times the pre-industrial level. In 2019 the global averaged mole fraction of CH_4 was 1877 ± 2 parts per billion (ppb) (WMO, 2020). Following a period of no growth from 2000 to 2006, the mole fraction of methane began to rise significantly in 2007 with growth worldwide, especially in the tropics and northern mid-latitudes (Nisbet et al., 2019). The causes driving this methane mole fraction rise are still not well understood and could be due to increased emissions or decline in the sinks of methane in the atmosphere.

Methane is emitted to the atmosphere by natural and anthropogenic sources. About two-thirds of methane is emitted by human activities and the remainder from natural sources (Saunois et al., 2016; Bridgham et al., 2013). The main natural sources of methane are wetlands, oceans, termites and clathrates (Dlugokencky et al. 2011). Anthropogenic methane sources include fossil fuel exploitation and distribution, ruminant animals, rice agriculture, landfill, wastewater management and biomass burning.

This study focuses on methane emissions in the State of Kuwait. Kuwait is a major oil producing country and its economy directly depends on export of crude and refined products. These activities are expected to result in the emission of gaseous pollutants to the atmosphere. There has been little research on methane emissions in Kuwait with the main focus on gas concentration, distribution and characterisation from oil and gas related activities (Al-Hamad and Khan, 2008; Al-Hamad et al. 2008a, b, 2009) and landfill sites (Al-Yaqout et al. 2005; Al-Ahmad et al. 2012; Al-Saffar and Al-Sarawi, 2018). All the previous studies have investigated a specific source and there have been no studies mapping the distribution of methane emissions across the country.

This research, for the first time in Kuwait, uses high-precision methane isotopic analysis of $\delta^{13}C_{CH4}$ coupled with World Meteorological Organisation (WMO) scale-calibrated mole fraction measurement in order to link isotopic signatures to methane emission sources. The study involves the use of mobile cavity ringdown spectroscopy (http://www.picarro.com) for methane plume identification in Kuwait and further analysis of Tedlar bag samples by isotope ratio mass spectrometry.

Methane stable isotopic analyses are used to identify and characterise sources, to gain better understanding of the gap between global methane budgets that result from bottom-up emission inventories and budget estimates from top-down observation (Zazzeri et al. 2015; Fisher et al. 2017). Methane emissions from sources such as gas leaks and landfills can span a wide range of $\delta^{13}C_{CH4}$ isotopic signatures (Schwietzke et al. 2016; Zazzeri et al. 2017). The $\delta^{13}C_{CH4}$ ratios enable distinction by providing insight into the methane origin. Atmospheric measurements of isotopic signatures can be used to apportion emissions from different sources. Methane emission inventories use "bottom-up" estimates of activity data and emission factors for individual methane sources. The total global emission estimated from the "bottom-up" methane inventory is about 30% larger than the "top-down" estimate calculated from direct measurements of methane in air (Saunois et al., 2016; Saunois et al., 2020; Jackson et al., 2020). Two inventories are available for Kuwait methane emissions, the international EDGAR inventory (Emissions Database for Global Atmospheric Research) (EC-JRC, 2019) and a local inventory (EPA, 2012 and EPA, 2019) of Kuwait's national communications under the United Nations Framework Convention on Climate Change (UNFCCC). Methane emissions estimations in both inventories comply with the Intergovernmental Panel on Climate Change (IPCC) Guidelines for National Greenhouse Gas Inventories (2006 Guidelines). The US NOAA measurement program includes greenhouse gas measurements from 204 sites in 45 countries. Unfortunately, there are very few greenhouse gas measurements in the Middle East region. In this study, methane measurements (mole fractions) are compared to flask measurements made by NOAA at the closest surface observation site in the Global Greenhouse Gas Reference Network (30°N, 35°E).

2. The research area: The State of Kuwait

The State of Kuwait covers an area of 17,818 km^2 at the northeastern end of the Arabian Peninsula (Fig. 1). It is located between latitudes 28°29′17.86″ and 30°7′22.57″ North and longitudes 46°32′7.2″ and 48°53′10.46″ East and consists of a mainland, where the capital Kuwait City is located, and nine uninhabited islands in the Arabian Gulf. The State of Kuwait is bounded to the south by Saudi Arabia and to the north and west by Iraq. The current population is approximately 4.5 million. The Kuwait urban area covers less than 7% of the country. Kuwait has a hyper-arid desert climate, hot and dry with a rainfall average ranging from 75 to 130 mm/year. Average daily temperature maxima range from 42 °C to 46 °C in summer with humidity exceeding 95% from mid-August to September. The prevalent wind direction is the west to north sector with annual average wind speed of 4.5–6 m/s, with a smaller but important component from the southeast (Neelamani et al., 2007; EPA 2012; WMO 2018; Kuwait Meteorological Center 2018; Yassin et al., 2018; see Supplementary Figures S1 and S2 for more detail).

The State of Kuwait is a major oil supplier with oil companies accounting for 95% of exports, 50% of gross domestic product (GDP) and 90% of government revenue. Kuwait holds approximately 101.5 billion barrels (bbl) of oil reserves, around 7% of the global oil total. Approximately 1.8 trillion cubic meters (m^3) of natural gas reserves have been proven (EPA 2012; OPEC ASB 2018).

In Kuwait, landfilling is the main disposal method for domestic waste (Al-Yaqout and Hamoda, 2002). Approximately 90% of all domestic waste is disposed in landfill sites and the remaining fraction is recycled. The landfill sites are not engineered, instead they are voids made by quarrying. The waste comprises household, organic, construction and industrial waste. Most of the landfill sites have been closed for more than 20 years due to operational problems, such as severe public health and environmental issues (Al-Ahmad et al., 2012; Al-Saffar and Al-Sarawi, 2018). There are 18 landfill sites in Kuwait state. Of these, 14 sites are closed and the other 4 are still operating and receiving municipal waste.

3. Materials and methods

Stable carbon isotopic analysis coupled with methane mole fraction measurements allow determination of the $\delta^{13}C_{CH4}$ source signature of emissions. The use of methane isotopic analysis as a tool that links methane emissions to specific sources of methane and for verifying inventories has been well demonstrated by several studies (Levin et al. 1999; Lowry et al., 2001; Fisher et al. 2006; Townsend-Small et al. 2012; Zazzeri et al. 2015, 2017; Brownlow et al. 2017; Lowry et al., 2020).

3.1. Air sample collection

In this study, air samples were collected using three different methods: 1) driving with a Picarro Mobile analyzer during a Kuwait field campaign (Fig. 2) over six consecutive days, 2) diurnal sampling from Al-Rabya urban area, and 3) regular (weekly) sampling over a two year period (2015 and 2016) from three sites in Kuwait. Some key potential emitting sites including the North oil field and sewage treatment plants were investigated further by collecting air samples within these restricted areas.

All samples were collected in 3-litre Tedlar bags (SKC Ltd) using a battery-operated micro diaphragm pump (NMP830KNDC - KNF Neuberger Ltd). The collected samples were shipped to the Greenhouse Gas Laboratory at Royal Holloway University of London (RHUL) for analysis.

3.2. Kuwait mobile methane measurement campaign

Investigation of methane sources required a dedicated sampling campaign which was carried out from 2nd to 7th May 2015, with a maximum recorded temperature of 42 °C during this period. Wind direction during the survey days reflected the dominant sectors from NW or SE and the average wind speed was 3.5 m/s. Before every survey, the wind direction was checked to verify that the expected intersection of emission plumes from potential source sites was accessible by road in the downwind area. During this campaign, different sites were visited in order to investigate potential methane sources such as landfills, sewage treatment plants, oil refineries, oil fields, and ruminant farms and markets.

Measurement of the methane (CH_4) mole fraction was conducted using a high-precision mobile Picarro G2301 CRDS analyser fitted into a 4WD vehicle (Fig. 2). The mobile Picarro system makes a new measurement of carbon dioxide (CO_2) and methane (CH_4) mole fractions every 3 s with negligible drift (see section 3.2.1). Methane plumes were measured while driving on public roads around the target sources. In this campaign various potential sources were investigated on the same day with air samples collected upwind to define background and downwind across the source plume. Further details on the Picarro instrument set-up and the Kuwait mobile campaign can be found in Zazzeri et al. (2015) and Al-Shalan (2019), respectively.

For urban areas with multiple methane sources, this method is particularly valuable (Phillips et al. 2013; Zazzeri et al. 2015, 2017). In order to properly visualise the methane mole fraction range, GIS ArcMap 10.2 software was used to generate maps displaying measured methane in ppm. Fig. 3 shows the route for all surveys covered during this campaign with locations of enhanced methane noted.

3.2.1. Instrument calibration

The Picarro 2301 CRDS instrument was calibrated in the RHUL Greenhouse Gas Laboratory against three WMO-scale referenced cylinders before it was shipped to Kuwait, two from National Oceanic and Atmospheric Administration (NOAA; http://www.esrl.noaa.gov/gmd/ccl/) and one from Max Planck Institute, Jena, and this was repeated after the instrument was returned to RHUL following the campaign. Precision for CH_4 was ±0.5 ppb and the drift in measurements between the two calibrations was small (less than 0.9 ppb).

3.3. Mole fraction and isotopic measurement of bag samples

Methane mole fraction in all Tedlar bag samples was measured using a Picarro G1301 Cavity Ring-Down Spectrometer in the RHUL Greenhouse Gas Laboratory. This instrument is calibrated using cylinders from Max Planck Institute, Jena, referenced to the WMO-2004A scale.

Continuous flow isotope-ratio mass spectrometry (CF-GC-IRMS) was used to analyse $\delta^{13}C$ of methane from the air samples using a modified

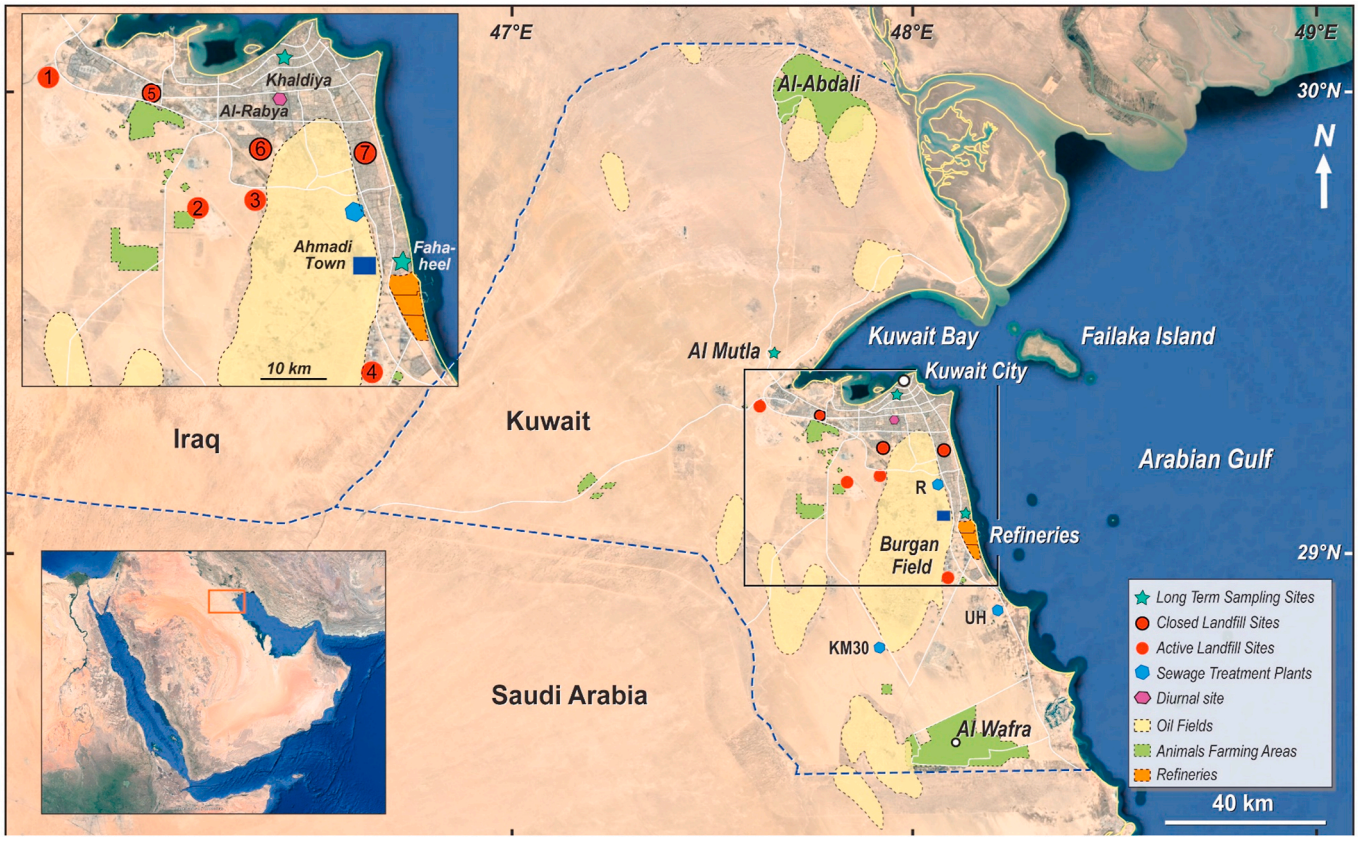

Fig. 1. Map of Kuwait showing the locations of methane sources (landfills, oil field, sewage, animal farms, refineries, Ahmadi town) and the three sites used in the long-term study. The map also shows the location of the diurnal measurement. The inset map shows the location of Kuwait. (COLORED).

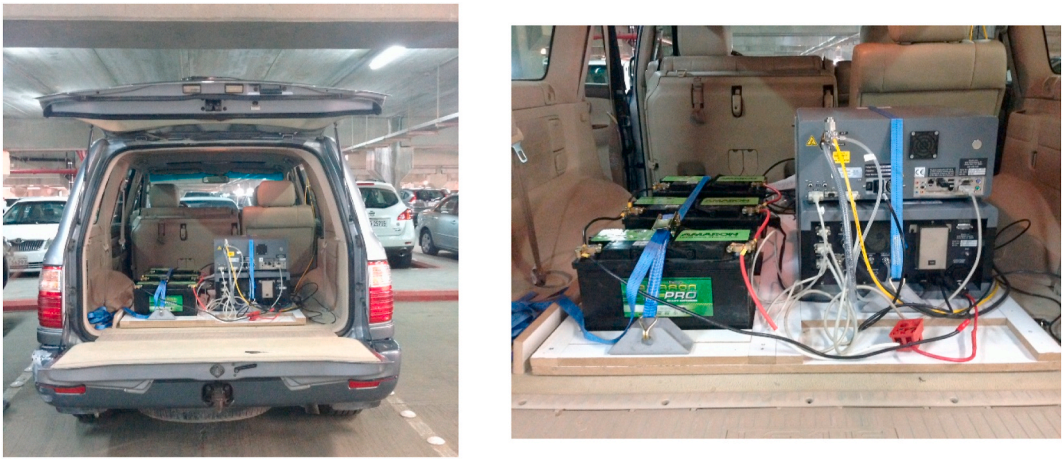

Fig. 2. Picarro Mobile Analyser System loaded in the vehicle used in the Kuwait sampling campaign. (COLORED).

Trace Gas preparation system and IsoPrime mass spectrometer, as detailed in Fisher et al. (2006). Measurements of atmospheric methane samples with mole fractions up to 7 ppm were carried out immediately without a dilution. However, air samples with higher mole fraction (>7 ppm), such as those from landfill boreholes or gas from the oil field, were first diluted with zero grade nitrogen (scrubbed of methane) to mole fractions between 2 and 5 ppm as that is the middle of the linear range for isotopic analysis.

3.4. Diurnal studies in Kuwait

Several diurnal studies were carried out during 2016 from the Al-Rabya urban area in Kuwait City in order to understand methane local sources by determining the isotopic signature of overnight build-up profiles. Air samples were collected in 3 L Tedlar bags every 2 h at 6 m AGL on the terrace of a house and analysed in the RHUL laboratory for methane mole fraction and $\delta^{13}C$.

3.5. Long term study

Three sampling sites were selected for weekly methane measurements in Kuwait during the two-year period January 2015 to December 2016 (see section 4.5). Methane measurement was carried out upwind (Al-Mutla site), in a desert area around 33 km northwest of Kuwait City. This site was chosen to isotopically characterise air coming from the eastern Mediterranean, Syria, and Iraq. The second sampling site is at Fahaheel (downwind sampling) that is located 35 km southeast of Kuwait City and 2 km west of the coastline at 2 m above the ground. The third sampling site was on the roof of the Department of Earth and Environmental Sciences at Kuwait University at 8 m above ground (Khaldiya). This site was chosen near to the center of Kuwait City to allow better understanding of urban CH_4 sources. The site is influenced by many potential methane sources such as landfills and a wastewater treatment plant. Samples were collected weekly from the three sites at approximately the same time. The collected air samples were then analysed at RHUL for CH_4 mole fraction and $\delta^{13}C$.

3.6. Data analysis

This research has followed the analysis described by Keeling (1958, 1961) and Miller and Tans (2003) to calculate the isotopic signature of each individual source and site. Many studies have successfully used Keeling and Miller-Tans plots to determine the $\delta^{13}C$ signature of a source in specific settings (e.g. Pataki et al. 2003; Rella et al. 2015; Zazzeri et al. 2015, 2017; Arata et al. 2016; Wang et al. 2018).

3.6.1. Keeling plot approach

The Keeling method (Keeling 1958, 1961) uses ^{13}C and CH_4 mole fraction measurements to determine the $\delta^{13}C_{CH4}$ isotopic signature of a source input in circumstances where there is a steady background and varying input proportion. The method has been used to interpret various sub-systems of the global carbon cycle (e.g. Keeling, 1958, 1961; Lowry et al., 2001; Pataki et al. 2003; Sturm et al. 2005; Fisher et al. 2006; Zazzeri et al. 2015, 2017; Lowy *et al.* 2020). In this study, the Keeling plot method was employed to calculate the isotopic signature of the methane source responsible for the excess inputs over an assumed constant background. This was achieved by plotting the $\delta^{13}C$ values (‰) (y-axis) against the inverse of methane mole fractions (ppm) ($1/CH_4$; x-axis) (Pataki et al. 2003). The isotopic signature of the source was interpreted from the regression line by the BCES method (Bivariate Correlated Errors and intrinsic Scatter) (i.e. Akritas and Bershady, 1996; Zazzeri et al. 2015). Following the Keeling plot approach, every methane source studied was assigned an isotopic signature (see section 4.6).

3.6.2. Miller-Tans approach

Miller and Tans (2003) have suggested an alternative approach for calculating isotopic signature from atmospheric measurements of CH_4 and $\delta^{13}C$. Unlike the Keeling plot method, the Miller-Tans method is more flexible and allows for straightforward specification of the background values of both CH_4 and $\delta^{13}C$. Hence, as described by Miller and Tans (2003) and Zazzeri et al. (2017), this approach becomes necessary when the background is not constant through the time or space relevant to the measurements. In this work, the Miller-Tans approach was used to calculate the $\delta^{13}C_{CH4}$ signature for the long-term study of three sites sampled during 2015 and 2016 that recorded seasonal changes in background (see section 4.5).

4. Survey results and source characterisation

A map of the measured methane mole fractions over the six days of mobile surveys is presented in Fig. 3. The main source hotspots were found to be landfill sites. Isotopic signatures of the CH_4 sources are summarized in Table 1. The baseline methane mole fraction during the mobile survey was consistently <2 ppm.

4.1. Landfill sites

Seven landfill sites were investigated in the mobile campaign, of which four sites are active (Al-Jahra landfill, the South Seventh Ring Road landfill, Kabad landfill and Mina Abdullah landfill) and three are closed sites (Al-Sulabiya landfill, Al-Qurain landfill and Jleeb Al-

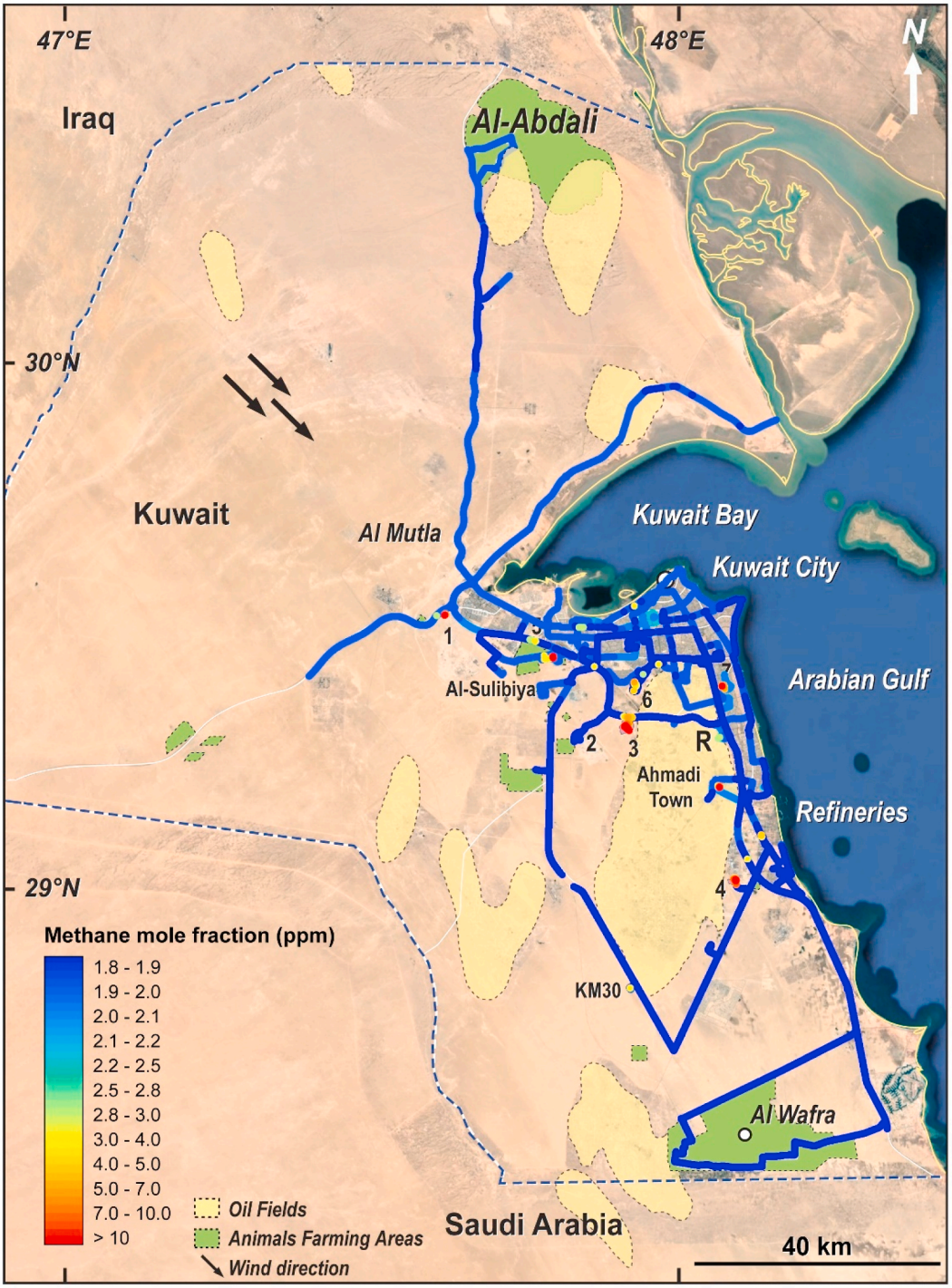

Fig. 3. GIS plot of methane mole fractions in ppm along the route of the 6 days of the Kuwait mobile campaign showing the locations of methane emissions. The map shows the landfill sites 1) Al-Jahra, 2) Kabad Construction, 3) South Ring Road, 4) Mina Abdullah, 5) Al-Sulaibiyah, 6) Jleeb Al-Shyoukh and 7) Al-Qurain. Oil fields are shown in pale yellow. Black arrows indicate the dominant wind direction during the survey period. The map was generated using Arc.Map10.2. Base map source: Esri, Digital Globe, GeoEye, Earthstar Geographics, CNES/Airbus DS, USDA, US GS, AEX, Getmapping, Aerogrid, IGN, IGP, Swisstopo, and the GIS User Community. (COLORED). (For interpretation of the references to colour in this figure legend, the reader is referred to the Web version of this article.)

Shuyoukh). The active landfill sites mainly receive household solid waste and emit significant amounts of methane, with the exception of the Kabad landfill that accepts only inert construction waste (see Supplementary Figure S3). The excess methane over background recorded off-site and on-site ranged from 1.6 ppm to 36.7 ppm. Methane isotopic signatures span a range from $\delta^{13}C_{CH4}$ -59.4 ± 1.4‰ to −51.9 ± 0.2‰, with an average $\delta^{13}C_{CH4}$ value of −56.6 ± 3.1‰ (1σ uncertainty). The average $\delta^{13}C_{CH4}$ signature of the three active uncovered landfills is −59.1 ± 0.5‰, whereas for the three closed covered landfill sites it is −54.2 ± 2.3‰. The difference is associated with methane oxidation within the soil cap of the covered closed landfill sites resulting in enriched $\delta^{13}C$ of methane emitted to the atmosphere (i.e. Liptay et al., 1998: Chanton et al., 1999: Zazzeri et al., 2015). Table 1 summarises the isotopic signatures identified from all the emitting landfill sites studied

Table 1
Methane isotopic signatures for different sources in Kuwait. * Wastewater treatment signatures are complicated because of variable processes across the sites: some of the keeling plots suggested two trends.

Methane source	Site	$\delta^{13}C$ (‰)
Landfills	Al-Jahra Landfill (Active)	-59.4 ± 1.4
	South Seven Ring Road (Active)	-58.5 ± 0.5
	Mina Abdullah (Active)	-59.5 ± 1.0
	Al-Sulaibiyah (Closed)	-51.9 ± 0.2
	Al-Qurain (Closed)	-54.3 ± 1.9
	Jleeb Al-Shuyoukh (Closed)	-56.4 ± 1.9
Fossil Fuel Extraction and Distribution	Al-Ahmadi Town (gas leakage)	-50.0 ± 0.2
	Refineries	-51.6 ± 0.5
	Ahmadi oil field (Greater Burgan)	-48.9 ± 0.2
Ruminants	Cow	-62.4 ± 0.4
	Sheep	-63.6 ± 0.1
	Camels	-60.0 ± 0.5
Wastewater Treatment Plants	Al-Riqqa (May 4, 2015)	-46.6 ± 0.03
		-50.5 ± 0.7*
	Al-Riqqa (January 7, 2016)	-45.1 ± 0.2
	Al-Riqqa (March 7, 2017)	-45.6 ± 0.1
		-50.7 ± 0.6*
	Kilo 30	-46.2 ± 0.1
	Um-Al-Himan (March 17, 2017)	-59.2 ± 0.9
		-46.8 ± 0.04*
Car Exhaust	Car parking	-13.1 ± 1.0

in Kuwait.

4.2. Fossil fuel extraction and distribution

To assign a representative $\delta^{13}C_{CH4}$ signature to emissions from natural gas, Kuwait Oil Company (KOC) allowed access to the North oil fields, but only to collect air samples for isotopic characterisation. The North oil fields include Sabriyah and Ar-Raudhatain fields. These fields were visited twice in March and October 2016 and 35 air samples were collected in 3 L Tedlar bags. Analysis of all air samples shows only small elevations of methane, with a narrow range of mole fractions between 1.91 and 2.08 ppm. The maximum mixing ratio was found downwind of the Booster installation, 2.02 ppm downwind of the Gathering Center and 2.01 ppm downwind of an active rig in Sabriyah oil field, but this excess over background was not high enough to calculate a $\delta^{13}C_{CH4}$ signature without large errors. A pure gas sample from the Burgan oil field to the south of Kuwait City gave a $\delta^{13}C_{CH4}$ signature of -48.9 ± 0.2‰.

Kuwait City itself has no urban gas distribution network, so no gas leaks were detected in the city. Just one area in Kuwait has underground gas distribution pipes, in Al-Ahmadi town. Three gas explosions occurred in 2010. Two occurred at different houses located in north Al-Ahmadi and connected to the KOC natural gas network. The third gas explosion however, occurred at a house in south Al-Ahmadi which was not connected to the KOC network (Alkhaledi et al., 2015). Al-Ahmadi town consists of many blocks. The so-called Block 1 has suffered from many natural gas leakages in the last decade (Al-Rashed, 2014). A mobile survey and sampling were carried out in Al-Ahmadi town residential area and identified gas leakage from an unknown source in Block 1. Many vents have been installed around Block 1 since 2010 to avoid dangerous underground build-up of methane. Maximum methane mole fraction measured was 9.01 ppm in Block 1 during the survey. The Keeling plot analysis based on the collected air samples shows that the $\delta^{13}C_{CH4}$ source signature is -50.0 ± 0.2‰. Based on this source signature, it is not possible to determine whether gas leakage is from the underground pipe network or natural geological seeps from the Burgan field.

Several measurement transects were conducted along the King Abdul-Aziz Highway, downwind of the oil refineries located along the coast SE of the city. Methane plumes were intercepted downwind of the west side of two of the refineries, carried inland by onshore breezes. The maximum methane mole fractions ranged from 2.7 ppm to 4.4 ppm. A Keeling plot analysis based on the collected air samples shows a $\delta^{13}C_{CH4}$ intercept value of -51.6 ± 0.5‰.

4.3. Sewage treatment

In this study, three wastewater treatment plants were investigated, Riqqa, KM30 and Umm Al-Hyman. There are several processes in which methane can be emitted to the atmosphere during sewage treatment, and these give different methane isotopic signatures. This variation of methane sources makes it difficult to have a distinct sewage $\delta^{13}C$ signature. Keeling plot analysis gives a wide range of $\delta^{13}C_{CH4}$ signatures between -59.2 and -45.1‰ as shown in Table 1, but with all but one area of one site in the range -51 to -45‰.

4.4. Ruminants

Livestock numbers in Kuwait State, according to the annual statistical bulletin 2015–2016 of the Public Authority of Agriculture and Fish Resources, were 29263 cattle, 588618 sheep, and 7718 camels, respectively (Table S1). Map Figs. 1 and 2 show the distribution of the livestock farming areas in Kuwait during 2015–2016. There are 20 times more sheep than cattle, but with an expected CH_4 emission that is close to 3 times the latter (57% compared to 21%, see Supplementary Section E) based on the methodology of Aljaloud et al. (2011) and using FAOSTAT data (http://www.fao.org/faostat/en/#data/GM).

The Picarro mobile survey identified methane plumes from local cows, sheep and camels, but not goats. The diet of the ruminants in Kuwait is a mixture of C3 plants and C4 plants with vitamins, most of which is imported. Cows were fed on green trefoil (C3), Ca in water with vitamins, malt (C3), corn with brown flour, silage, rape seed and soya beans. Camels and sheep in Kuwait are fed a mix of both C3 and C4 plants, such as hay, barley, bran, and grass. The maximum methane mole fractions were recorded inside one of the animal farms in the Al-Sulabiya area, the Shahab Al-Deen cattle farm, where methane mole fraction reached 19.2 ppm next to a barn. Eight samples were collected upwind and downwind of this farm. A $\delta^{13}C$ source signature of -62.4 ± 0.4‰ was calculated from analysis of the collected air samples.

Al-Mawashi sheep farm, one of the biggest Kuwait livestock farms was also surveyed. A maximum methane mole fraction of 2.3 ppm was recorded, with a Keeling plot intercept of $\delta^{13}C_{CH4}$ -63.6 $\pm$ 0.1‰.

A group of 200 camels were grazing next to a public road. Emissions were detected downwind with maximum methane mole fraction of 2.16 ppm, elevated enough above the background of 1.89 ppm to give a calculated Keeling plot intercept of -60.0 ± 0.5‰.

4.5. Long term measurements

Seasonal changes in the methane mixing ratio were observed from the three regular sampling sites, which are close to stations of the Kuwait Meteorological Department (met.gov.kw). A significant difference is observed between summer and winter methane mole fractions. The meteorological conditions play an important role in pollutant distribution affecting the ground level mole fractions in the residential areas (Al-Azmi et al., 2009). Methane mole fractions reach minimum values in summer as increased wind turbulence and a high inversion layer influence dispersion. The reaction with hydroxyl radicals (OH) is the main sink of methane and is also enhanced in summer. This exerts a fractionation effect on methane $\delta^{13}C$ (Nisbet et al., 2016; Zazzeri et al., 2017). In the extra-tropical northern hemisphere, methane mole fractions tend to be highest in November and December (Zhou et al., 2004). This is partly due to lower boundary layer heights in autumn and winter and calmer meteorological conditions (Worthy et al., 1998; Levin et al.,

1999; Zhou et al., 2004; Al-Azmi et al., 2009; Zazzeri et al., 2015). For the period 2015 and 2016, mean winter season methane mole fractions are around 90 ppb higher than the summer values (Fig. 4).

Long term measurements of methane mole fraction combined with stable carbon isotopic composition are used to determine a mean $\delta^{13}C_{CH4}$ source signature that characterises the region and hence allows estimation of the proportion of the main CH_4 sources in a source mix. Fig. 4 shows measured $\delta^{13}C$ in 2015 and 2016 for the three investigated sites in Kuwait. Seasonal variations were observed in $\delta^{13}C_{CH4}$. The mean amplitude was ±0.4‰, with most depleted values down to −49.9‰ associated with maximum methane mole fractions, indicating that most CH_4 emissions in the region are isotopically lighter than background atmospheric CH_4 (i.e.Yamada et al., 2005). Two outliers were observed in 2015 and 2016 from the Fahaheel site, out of 280 samples collected across three sites. These outliers have a high methane mole fraction but are not depleted in $\delta^{13}C_{CH4}$.This might be due to defective sample bags but could record input from a local combustion source near to the site.

The isotopic signature of the source mix was calculated for all three

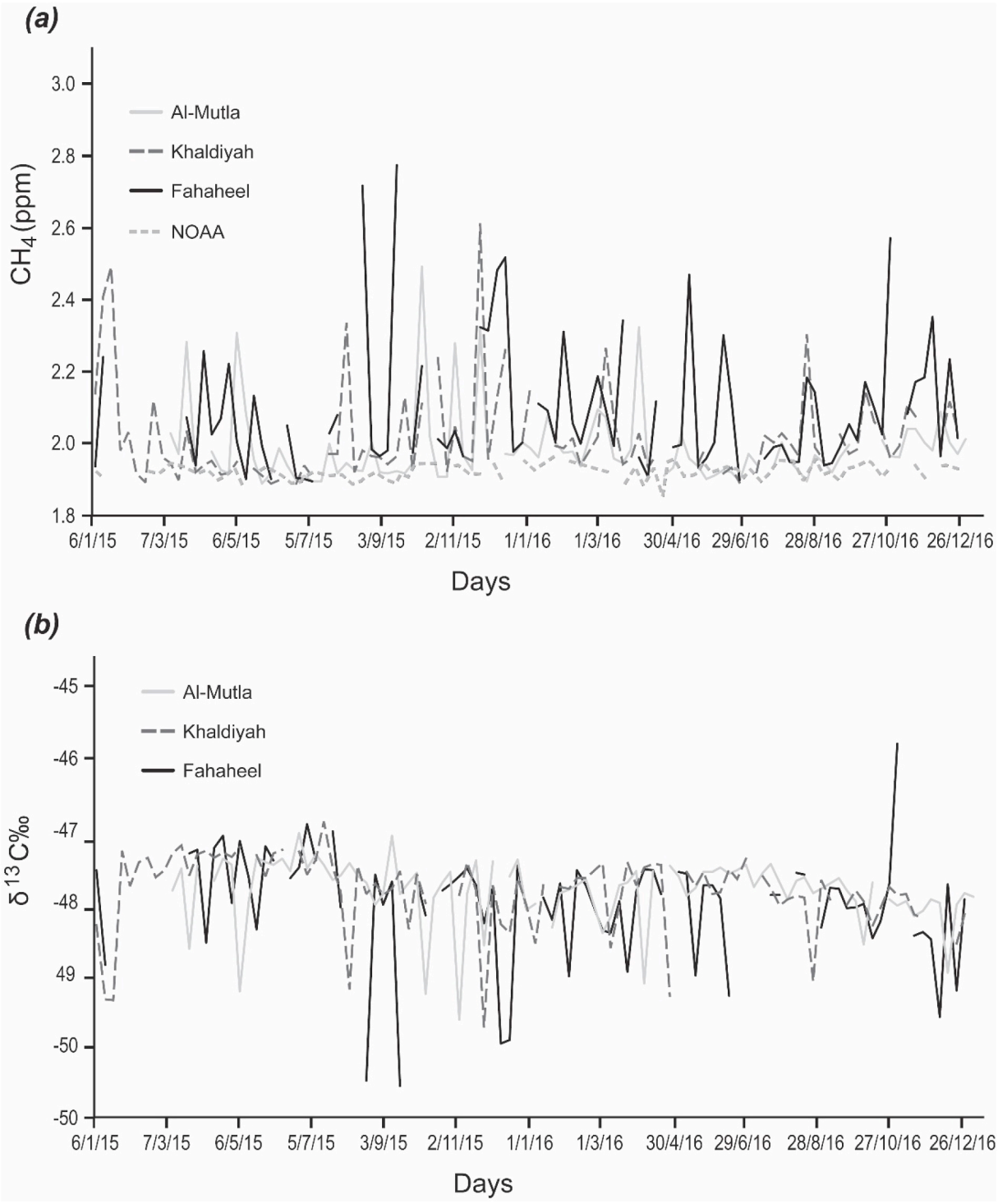

Fig. 4. Long term measurements for the period 2015 and 2016 for three sites in Kuwait, (a) methane mole fraction of the three sites compared to the closest NOAA site. (b) methane isotopic measured values for the three sites.

sites combined during 2015 and 2016 using a different background value for each season. Fig. 5 shows the source signature calculated using a Miller-Tans plot and the overall $\delta^{13}C_{CH4}$ source mix for Kuwait is -55.9 ± 0.7‰.

4.6. Diurnal measurement

Three diurnal studies were carried out in the Al-Rabya urban area during 2016 to determine the mean $\delta^{13}C_{CH4}$ source signature characterising this region of the city and hence identify the main methane sources.

The first diurnal study took place on 5th – 6th January 2016 when air samples were collected every 2 h over 24 h. Based on the collected air samples, the Keeling plot shows a $\delta^{13}C_{CH4}$ intercept of -56.1 ± 0.9‰. Methane built-up overnight with a maximum mole fraction of 5.7 ppm at midnight, and an associated drop of the wind speed from 1.7 m/s to 0.7 m/s, and dissipated in the morning as the air mixed.

The second diurnal sampling campaign was carried out on 18th – 19th July 2016. The sampling started at 3 p.m. with an easterly wind direction caused by the sea breeze coming from Kuwait coast (Al-Sarraf et al., 2019). The wind changed to a southerly by early morning with maximum methane mole fraction of 4.8 ppm corresponding to minimum measured $\delta^{13}C$ of -54.1 ± 0.04‰. The intercept of the Keeling plot gives $\delta^{13}C_{CH4}$ -58.2 $\pm$ 0.4‰, suggesting a dominantly biogenic source.

The last diurnal study was carried out in autumn, 17th – 18th October 2016. Air samples were collected every 2 h over 24 h. Fig. 6a shows the Keeling plot based on the collected samples, giving a $\delta^{13}C_{CH4}$ signature of -59.3 ± 0.3‰, which is more ^{13}C-depleted than the previous diurnal studies. The study was started at 3 p.m. when the wind direction was N to NW for the first 4 h then it turned to a southerly wind direction. This southerly air mass measured during the evening and early morning contained methane (peaking at 6.9 ppm) that is highly depleted in ^{13}C, which can be attributed to a prevalent biogenic component in methane emissions such as landfills (Fig. 6b).

5. Discussion

5.1. Kuwait methane measurements compared to NOAA baseline observation

The closest NOAA/ESRL/GMD station for which methane mole fractions is measured in flask samples is located at 29.96°N and 35.06°E to the west of Kuwait, and is the only long-term station within the Kuwait air mass footprint (see Supplementary Fig. S4). It is in the dominant upwind air mass corridor for Kuwait and representative for up to 52% of daily back trajectories (Fig. 7). The calculation of the air movement during 2015 and 2016 for each sampling day shows that 76% of the air masses are coming from a 90° sector between WNW and NNE directions passing through Jordan, Syria, Iraq and SW Iran (Fig. 7). Some of these air masses pass over Cyprus and the eastern Mediterranean region (Fig. S4). Additionally, 16% of trajectories bring air from Iran (NE) and 8% from the Arabian Gulf (SE). There were no trajectories crossing the entirety of the Arabian Peninsula, although the final approach to the Kuwait sampling sites of a small number of air masses was from the SSE – W sector. In this study, the Kuwait 2-year measurements of methane mole fraction from three sites for 2015 and 2016 were compared to the weekly flask measurements from the NOAA sampling site (Fig. 4), highlighting the trend and seasonal variation. The average background methane mole fraction for the NOAA site is 1.89 ppm, which is similar to the Kuwait background of 1.90 ppm for the period 2015 and 2016. All sites show the minimum mole fractions in May and June and maxima in November. There is a good agreement between the baseline measurements in 2015 and 2016 at all three Kuwait sites and the NOAA site over the same period, validating the changing background signals chosen to produce the Kuwait Miller-Tans plot.

5.2. Evaluation of the EDGAR emissions and EPA database for Kuwait

The Emissions Database for Global Atmospheric Research (EDGAR) report emission estimates for the major sources of anthropogenic methane, such as: fossil fuel, livestock and solid waste (EC-JRC 2019). EDGAR version 5.0 is a comprehensive database of anthropogenic emission time series from 1970 until 2015 for the GHGs that use the IPCC sectoral classification. The data are represented per source category at both country/region levels, as well as on grid basis. The bottom-up estimation by EDGAR is based on statistics multiplied by specific emission factors.

EDGAR estimates that fugitive emissions from oil and gas are the dominant source of methane emissions for Kuwait making up 85%–62% of the total methane emissions depending on inventory years. This could be an overestimate as the new measurements (see section 4.2), showed no evidence for significant methane emissions from the oil fields during the drive through the Burgan oil fields in 2015, or from air samples collected in the Northern oil fields. EDGAR 5.0 places 78% of oil and gas fugitive methane emissions in fields to the SW of the country (Fig. 7), but mobile surveys were not downwind of these fields due to the dominant air movement, and neither were the 3 long-term sites. Flaring density

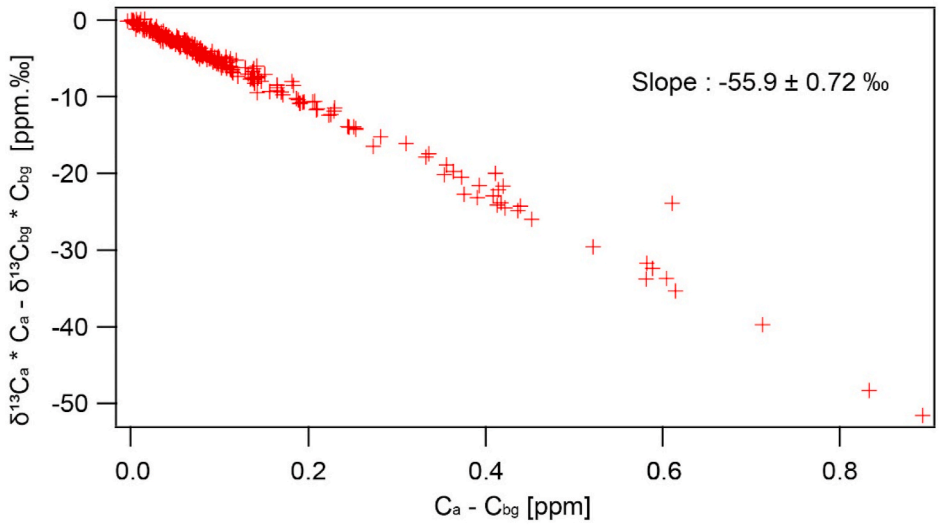

Fig. 5. Miller -Tans plot based on all the isotopic values measured in Kuwait during the period from 2015 to 2016. (COLORED).

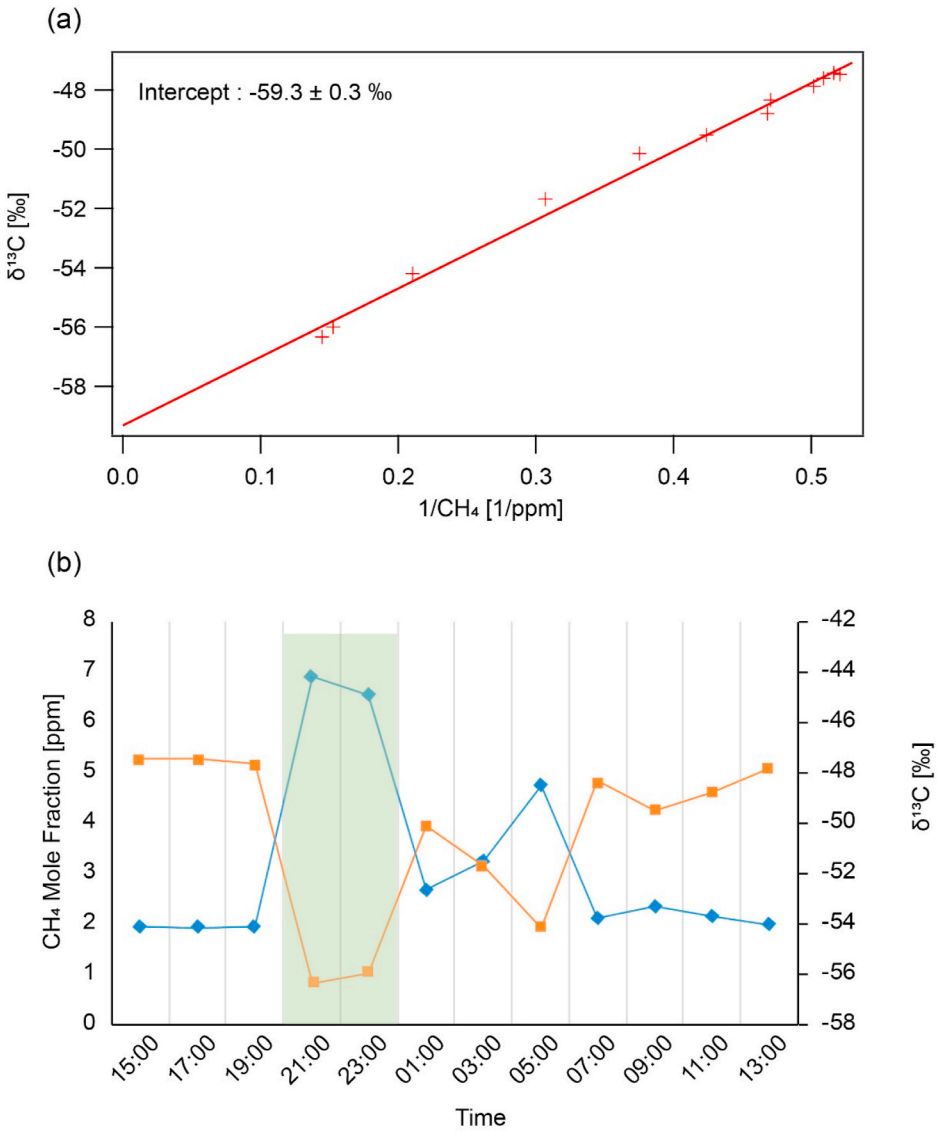

Fig. 6. (a) Keeling plot based on samples collected in Al-Rabya urban area on 17thand 18th October 2016. (b) Methane mole fractions and $\delta^{13}C$ measured in Al-Rabya urban area 17th and 18th October 2016, the blue line represents methane mole fractions, orange line is $\delta^{13}C$ and green shaded zone shows that the highest CH_4 mole fraction sample has a ^{13}C-depleted signature. (COLORED). (For interpretation of the references to colour in this figure legend, the reader is referred to the Web version of this article.)

based on radiative heat data from Fig. 7 suggests that one of these fields could emit significant methane if flaring is inefficient, but that other EDGAR inventory hotspots may not be so significant. The northern and Burgan oil fields are seen as notable areas of flaring, but survey data suggest that these are not translating into measurable increases in excess CH_4 over background.

Kuwait's Initial National Communications (INC) under the United Nations Framework Convention on Climate Change (UNFCCC) in 2012 was the first greenhouse gas emission inventory for Kuwait, focusing on emissions published by the Environment Public Authority (EPA) of Kuwait (EPA, 2012). This inventory followed the IPCC 1996 guidelines in development and used 1994 as the base year. The inventory estimated that 70.4% of Kuwait methane was derived from fugitive emissions from fossil fuels, 26.2% from waste and 2.1% from agriculture. The waste sector was entirely landfill emission with no wastewater treatment emissions. The uncertainties in this UNFCCC 1994 base year report associated with estimation of GHG emissions and removals in Kuwait are due to data gaps, quality issues, and inconsistencies across different sources.

Kuwait's second national communications SNC compiled an update to its inventory (July 2019) of greenhouse gas emissions for the base year 2000. Kuwait's (SNC) shows different results to the INC and is in better agreement with this measurement study. This second inventory estimates 81% of Kuwait methane emissions to be derived from waste, 8% livestock and 7% from fossil fuel emissions, with the remainder being 3% transportation and 1% electrical. EPA 2019 agrees with new measurements that the main sources of methane emissions in Kuwait are biogenic resulting from the waste sector as shown in Table 2.

5.3. *Verification of Kuwait inventory*

A mean $\delta^{13}C_{CH4}$ isotopic signature for each methane source category was calculated (Table 2), in order to verify the inventory (see details of the calculations in Supplementary Section E). Table 2 shows the source apportionment of methane emissions from inventories and the isotopic signatures of the source mix calculated for each inventory based on the % of each source in the inventory. Use of mass balance was attempted to calculate an appropriate source mix for Kuwait to match the representative mean source mix of −55.9‰ identified for combined 3-site, 2-year record by the Miller-Tans method (see section 4.5) including addition of an observed sewage component (Table S5).

The overall regional source mix calculated for Kuwait using the EDGAR v5.0 inventory for the years 1994, 2012 and 2015 is much more enriched, with $\delta^{13}C_{CH4}$ signatures of −51.2, −52.7 and −52.8‰, respectively. This change is due to a reduction from 85.3 to 62.8% of methane emissions from the fossil fuel sector over this period, and a

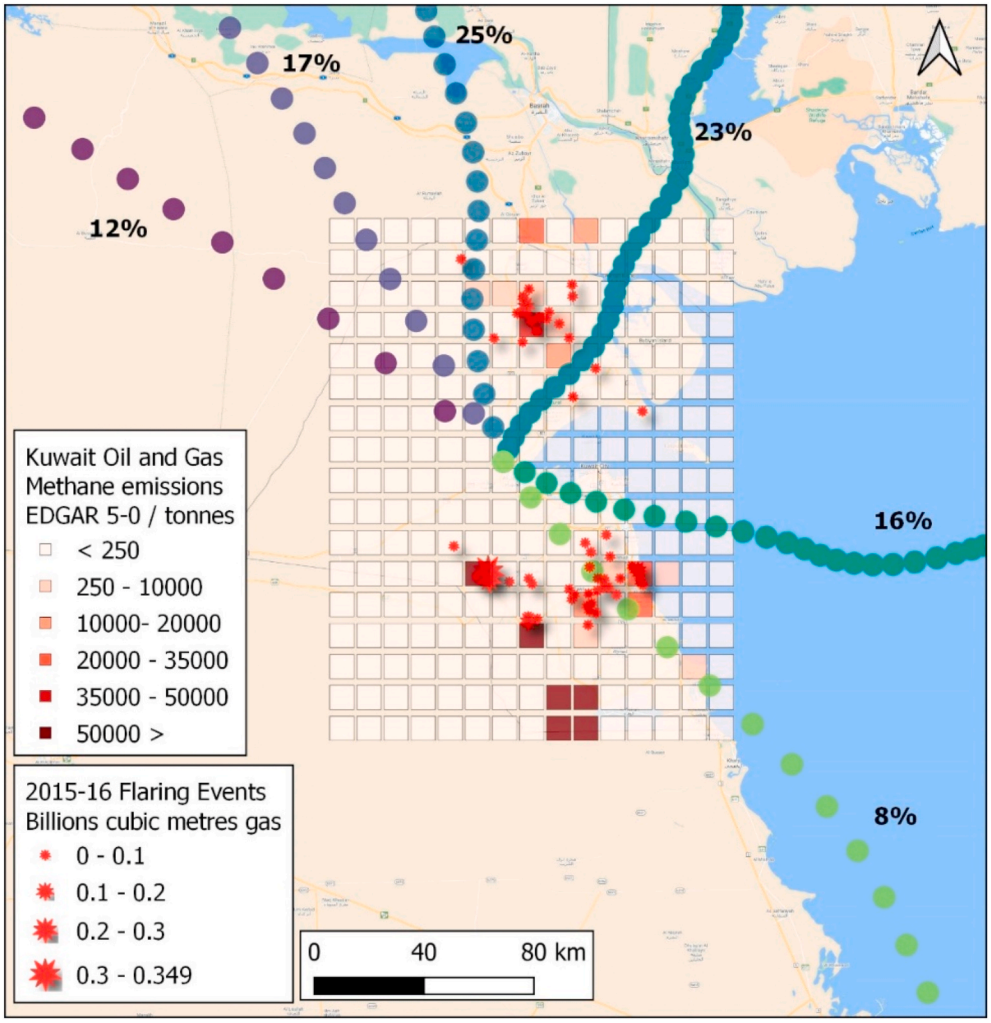

Fig. 7. Kuwait oil and gas methane emissions from EDGAR inventory data and flaring events during 2015–2016 from https://viirs.skytruth.org/apps/heatmap/flarevolume.html#. Back trajectories arriving at Jal Aliyah station are determined by HYSPLIT driven with NCEP re-analysis meteorology for every 12 h throughout 2015–2016. The trajectories are clustered into 5 dominant directions with each colored circle representing an hour of time on each of the mean trajectories. The dominant flow of air is from the Northerly sectors, with air having passed through the major oil and gas fields in the north and SE of Kuwait on route to the measurement sites. (COLORED).

Table 2
Methane emissions as percentages for the main source categories from Kuwait EPA and EDGAR version v5.0 and calculated $\delta^{13}C$ signatures of the emission mix. Source category signatures explained in Supplementary Section F.

Inventory	Fossil Fuel (%)	Landfills (%)	Sewage (%)	Animals (%)	Combustion (%)	$\delta^{13}C_{CH4}$ signature of Source mix (‰)
EPA 2012	70.4	26.2	0	2.1	1.3	−51.9
EDGAR, 1994	85.3	13.2	1.1	0.2	0.2	−51.2
EDGAR, 2012	68	28.8	2.5	0.5	0.3	−52.7
EDGAR, 2015	62.8	33.6	2.7	0.6	0.3	−52.8
EPA 2019	7	81	0	8	4	−56.0
δ^{13} CH_4 (‰) of sources from measurement	−50	−58	−49	−63.6	−16	Miller-Tans[a] −55.9

[a] Calculated using the Miller-Tans method (see Fig. 5).

corresponding increase from 14.3 to 36.3% derived from the waste disposal and treatment sector. These signatures are similar to the Kuwait EPA 2012 inventory that gives −51.9‰ for the calculated source mix. The Kuwait EPA 2019 inventory on the other hand gives an estimated $\delta^{13}C_{CH4}$ for the source mix of −56.0‰. Calculations using the earlier EDGAR 4.3 database are shown in Table S5 for comparison. EDGAR 5.0 suggests that 78% of 823 kT of methane emissions from oil and gas infrastructure are from only 6 of 194 0.1 × 0.1° grid squares that cover the country (Fig. 7). If this 78% of fossil fuel emissions from SW oilfields, that are outside of the air mass footprint of the mobile and fixed measurement sites, are excluded from the 2015 calculation then a signature of −55.2‰ is within error of the Miller-Tans signature of −55.9‰.

The overall regional source mix based on long-term measurements over two years is far more ^{13}C depleted than calculations using either EDGAR or the earlier EPA inventories. This suggests that the majority of the fugitive methane emitted in the footprint of mobile and fixed site measurements is derived from biogenic sources such as landfills. This is supported by the Kuwait mobile campaign observations that aimed to identify the main sources of methane emissions in Kuwait and found that landfills are the main source for methane emissions with an average isotopic signature of −58‰.

EPA 2019 agrees that the main source of methane emissions in Kuwait is biogenic methane from the waste sector. As shown in (Table 2) the isotopic mass balance giving $\delta^{13}C_{CH4}$ of −56.0‰ based on EPA 2019 is in close agreement with the −55.9‰ identified by Miller-Tans plots. But this presumes that the waste emission is all from landfill. However significant emissions from wastewater treatment were observed during the mobile campaign measurements which are not included in the EPA

2019 inventory and these are more enriched in ^{13}C compared to landfills, so some revision of the EPA inventory is required.

The findings are valid for the large proportion of the country that could be covered by the mobile measurement surveys or that is in the sphere of influence of the air mass trajectories arriving at the 3 long-term measurement sites during 2015 and 2016. The contribution of fossil fuel emissions in the EDGAR database does not agree with the Kuwait National Inventory or the KOC suggestions that flaring is greatly reduced. The remoteness and lack of access to the SW oil fields combined with prevailing wind directions mean that neither long-term fixed site or mobile surveys as in this study, or further distant ship surveys (e.g. Paris et al., 2021) will confirm if these fields are major methane emitters and aerial surveys by small aircraft downwind of these fields (e.g. France et al., 2021), backed up by satellite information, are needed to resolve this. Further ground or airborne studies are required in the middle-eastern region to resolve mismatches between inventory data, evidence for flaring and fossil fuel company reporting.

6. Conclusions and recommendations

6.1. Conclusions

This research demonstrates for the first time in Kuwait that continuous mobile measurements for plume identification coupled with high-precision isotopic analysis is an effective way of identifying methane sources and understanding their relative contributions. To unambiguously quantify relative contributions will require further work, particularly in the SW region of the country, utilizing aircraft and/or satellite retrievals. The results of this study will contribute to understanding the methane budget of this poorly studied region.

This study found that the main source of methane emissions in the upwind footprint of the ground surveys, or long-term measurement sites, are the landfill sites, and the expected high emissions from oil production sites were not seen, although there were some measured emissions from oil refineries, and from Ahmadi Town, the only area of Kuwait with a gas distribution network.

In recent years KOC have reported a great reduction in flaring (Figure S5), instead using this to provide its power plants with gas supplies to meet a rapidly growing electricity demand. Over the last five years (2014–2018), they suggest that the remaining gas flaring volumes were reduced by about 40 per cent (United Nations, 2020). The isotopic mass balance for 2015–2016 also suggests that the proportion of methane emission from fossil fuel extraction and distribution within the measurement footprint is low. Either these large reductions in methane emissions from fossil sources are not yet fully recognized in the EDGAR database, or the EDGAR fossil fuel emissions are real and require airborne surveys to resolve areas where there is no ground accessibility.

6.2. Recommendations for future studies and mitigation of methane emissions in the Middle East

This study has the potential to be extended to other countries in the region that follow similar landfill and fossil fuel extraction and distribution practices but may not have verification of inventories. The long-term high precision measurement of methane mole fraction and $\delta^{13}C$ in Kuwait should be repeated to be able to evaluate future changes in the sources and to assess the effect of mitigation strategies. Moreover, a further mobile survey should be carried out with a more recently-available instrument to measure ethane as this would be another way of a distinguishing thermogenic fossil fuel sourced methane from biogenic methane.

In European countries, waste segregation and landfill management with collection of gas from landfills (waste to energy) has been very successful in reducing emissions. In some cases, energy generation from landfill gas is an important source of income for the waste companies. Hence, implementation of similar technologies in Kuwait would greatly reduce emissions. Mobile campaigns demonstrated that all studied sewage treatment plants emit some methane to the atmosphere, but the Kuwait EPA inventories do not include sewage methane emissions, so these should be assessed for future inventory revisions.

CRediT authorship contribution statement

A. Al-Shalan: Conceptualization, Funding acquisition, Project administration, Investigation, Formal analysis, Validation, Writing – original draft, Data curation. **D. Lowry:** Conceptualization, Funding acquisition, Project administration, Methodology, Investigation, Formal analysis, Supervision, Validation, Writing – review & editing. **R.E. Fisher:** Methodology, Formal analysis, Supervision, Validation, Writing – review & editing. **E.G. Nisbet:** Funding acquisition, Supervision, Writing – review & editing. **G. Zazzeri:** Methodology, Investigation, Formal analysis, Writing – review & editing. **M. Al-Sarawi:** Investigation, Supervision, Writing – review & editing. **J.L. France:** Methodology, Formal analysis.

Declaration of competing interest

The authors declare that they have no known competing financial interests or personal relationships that could have appeared to influence the work reported in this paper.

Acknowledgements

This research forms part of the PhD thesis of A. Al-Shalan. The project was partially funded by the Kuwait Foundation for the Advancement of Sciences (KFAS) under project code “P115–64SC-01”, which covered the Kuwait campaign survey, regular sampling, and analytical costs. UK investigators working on data analysis were supported by two UK National Environment Research Council Projects, NE/P019641/1 New methodologies for removal of methane and NE/N016238/1 MOYA the Global Methane Budget 2016–2020. Eng.Salah Al-Ansari, the acting director of the Meteorological department, Directorate General Civil Aviation of Kuwait State, and Dr. Hassan Aldashti, climatology superintendent, are thanked for producing the wind roses in the supplementary information.

Appendix A. Supplementary data

Supplementary data to this article can be found online at https://doi.org/10.1016/j.atmosenv.2021.118763.

References

Akritas, M.G., Bershady, M.A., 1996. Linear regression for astronomical data with measurement errors and intrinsic scatter. Astrophys. J. 470, 706–714.

Al-Ahmad, M., Dimashki, M., Nassour, A., Nekkes, M., 2012. Characterization , concentrations and emission rates of volatile organic compounds from two major landfill sites in Kuwait. J. Am. Sci. Environ. Publ. Sci. 8, 56–63.

Al-Azmi, B.N., Nassehi, V., Khan, A.R., 2009. SO_2 and NOx emissions from Kuwait power stations in years 2001 and 2004 and evaluation of the impact of these emissions on air quality using industrial sources complex short-term (ISCST) model. Water Air Soil Pollut. 203, 169–178. https://doi.org/10.1007/s11270-009-0001-4.o.

Al-Hamad, K.K., Khan, A.R., 2008. Total emissions from flaring in Kuwait oilfields. Am. J. Environ. Sci. 4, 31–38. https://doi.org/10.3844/ajessp.2008.31.38.

Al-Hamad, K.K., Nassehi, V., Khan, A., 2008a. Impact of green house gases (GHG) emissions from oil production facilities at northern Kuwait Oilfields : Simulated Results Department of Chemical Engineering Loughborough University. In: Coastal and Air Pollution Division, vol. 4. Kuwait Institute for Science, pp. 491–501.

Al-Hamad, K.K., Nassehi, V., Khan, A., 2009. Methane and other hydrocarbon gas emissions resulting from flaring in Kuwait oilfields. Recent Adv. Technol. 601–618.

Al-Hamad, K.K., Nassehi, V., Khan, A.R., 2008b. Methane and other hydrocarbon gas emissions resulting from flaring in Kuwait oilfields. Int. J. Civ. Environ. Eng. 2, 144–152.

Aljaloud, A.A., Yan, T., Abdukader, A.M., 2011. Development of a national methane emission inventory for domestic livestock in Saudi Arabia. Anim. Feed Sci. Technol. 166–167, 619–627. https://doi.org/10.1016/j.anifeedsci.2011.04.044.

Alkhaledi, K., Alrushaid, S., Almansouri, J., Alrashed, A., 2015. Using fault tree analysis in the Al-Ahmadi town gas leak incidents. Saf. Sci. 79, 184–192. https://doi.org/10.1016/j.ssci.2015.05.015.

Al-Rashed, A., 2014. Detection of Natural gas leakage in Al-Ahmadi area, South of Kuwait: A preliminary study. Nat. Sci. 12, 87–93.

Al-Saffar, A., Al-Sarawi, M., 2018. Geo-visualization of the distribution and properties of landfill gases at Al-Qurain landfill , Kuwait. Kuwait J. Sci. 45, 93–104.

Al-Sarraf, H., Broeke, M.V.D., Al-Jassar, H., 2019. Effexts of the sea breeze circulation on soil temperature over Kuwait using in situ observations and the ECMWF model. Open Atmos. Sci. J. 2019 (13), 29–42. https://doi.org/10.2174/1874282301913010029.

Al-Shalan, A., 2019. Methane Emissions in Kuwait: Plume Identification, Isotopic Characteriation & Inventory Verification. Unpublished doctoral thiess. Royal Holloway, University of London, p. 258.

Al-Yaqout, A.F., Hamoda, M.F., 2002. Report: management problems of solid waste landfills in Kuwait. Waste Manag. Res. 20, 328–331. https://doi.org/10.1177/0734247X0202000403.

Al-Yaqout, A.F., Hamoda, M.F., Zafar, M., 2005. Characteristics of wastes, leachate, and gas at landfills operated in arid climate. Pract. Period. Hazard. Toxic, Radioact. Waste Manag. 9, 97–102. https://doi.org/10.1061/(ASCE)1090-025X(2005)9:2(97).

Arata, C., Rahn, T., Dubey, M.K., 2016. Methane isotope instrument validation and source identification at four corners, New Mexico, United States. J. Phys. Chem. 120, 1488–1494. https://doi.org/10.1021/acs.jpca.5b12737.

Bridgham, S., Cadillo-Quiroz, H., Keller, J.K., Q, Z., 2013. Methane emissions from wetlands : biogeochemical , microbial , and modeling perspectives from local to global scales. Global Change Biol. 19, 1325–1346. https://doi.org/10.1111/gcb.12131.

Brownlow, R., Lowry, D., Fisher, R.E., France, J.L., Lanoisellé, M., White, B., Wooster, M. J., Zhang, T., Nisbet, E.G., 2017. Isotopic ratios of tropical methane emissions by atmospheric measurement. Global Biogeochem. Cycles 31, 1408–1419. https://doi.org/10.1002/2017GB005689.

Chanton, J.P., Rutkowski, C.M., Mosher, B., 1999. Quantifying methane oxidation from landfills using stable isotope analysis of downwind plumes. Environ. Sci. Technol. 33, 3755–3760. https://doi.org/10.1021/es9904033.

Dlugokencky, E.J., Nisbet, E.G., Fisher, R., Lowry, D., 2011. Global atmospheric methane: budget, changes and dangers. Phil. Trans. Math. Phys. Eng. Sci. 369, 2058–2072. https://doi.org/10.1098/rsta.2010.0341.

EC-JRC, EDGAR v5.0 Greenhouse Gas Emissions, 2019. European commission, joint research centre (EC-JRC) [Dataset], PID. http://data.europa.eu/89h/488dc3de-f072-4810-ab83-47185158ce2a.

Environment Public Authority (EPA), 2012. Kuwait's Initial National Communications under the United Nations Framework Convention on Climate Change. Kuwait.

Environment Public Authority (EPA), 2019. Kuwait's Second National Communications under the United Nations Framework Convention on Climate Change. Kuwait.

Fisher, R.E., France, J.L., Lowry, D., Lanoisellé, M., Brownlow, R., Pyle, J.A., Cain, M., Warwick, N., Skiba, U.M., Drewer, J., Dinsmore, K.J., Leeson, S.R., Bauguitte, S.J.B., Wellpott, A., O'Shea, S.J., Allen, G., Gallagher, M.W., Pitt, J., Percival, C.J., Bower, K., George, C., Hayman, G.D., Aalto, T., Lohila, A., Aurela, M., Laurila, T., Crill, P.M., McCalley, C.K., Nisbet, E.G., 2017. Measurement of the ^{13} C isotopic signature of methane emissions from northern European wetlands. Global Biogeochem. Cycles 31, 605–623. https://doi.org/10.1002/2016GB005504.

Fisher, R., Lowry, D., Wilkin, O., Sriskantharajah, S., Nisbet, E.G., 2006. High-precision, automated stable isotope analysis of atmospheric methane and carbon dioxide using continuous-flow isotope-ratio mass spectrometry. Rapid Commun. Mass Spectrom. 20, 200–208. https://doi.org/10.1002/rcm.2300.

France, J.L., Bateson, P., Dominutti, P., Allen, G., Andrews, S., Bauguitte, S., Coleman, M., Lachlan-Cope, T., Fisher, R.E., Huang, L., Jones, A.E., Lee, J., Lowry, D., Pitt, J., Purvis, R., Pyle, J., Shaw, J., Warwick, N., Weis, A., Wilde, S., Witherstone, J., Young, S., 2021. Facility level measurement of offshore oil and gas installations from a medium-sized airborne platform: method development for quantification and source identification of methane emissions. Atmos. Meas. Tech. 14, 71–88. https://doi.org/10.5194/amt-14-71-2021.

Intergovernmental Panel on Climate Change (IPCC), 1996. Revised 1996 IPCC Guidelines for National Greenhouse Gas Inventories. https://www.ipcc.ch/report/revised-1996-ipcc-guidelines-for-national-greenhouse-gas-inventories/.

Jackson, R.B., Saunois, M., Bousquet, P., Canadell, J.G., Poulter, B., Stavert, A.R., Bergamaschi, P., Niwa, Y., Segers, A., Tsuruta, A., 2020. Increasing anthropogic methane emissions arise equally from agricultural and fossil fuel sources. Environmrntak Research Letters 15. https://doi.org/10.1088/1748-9326/ab9ed2.15.07.2020.

Keeling, C.D., 1958. The concentration and isotopic aboundances of carbon dioxide in the atmosphere. Geochem. Cosmochim. Acta 13, 322–334.

Keeling, C.D., 1961. The concentration and isotopic aboundances of carbon dioxide in rural and marine air. Geochem. Cosmochim. Acta 24, 277–298.

Kuwait Meteorological Centre. Directorate general of Civil aviation. Climate history. [Online]. Available at: http://www.met.gov.kw/Climate/climate_hist.php?lang=engwww.met.gov.kw. (Accessed April 2015).

Levin, I., Glatzel-Mattheier, H., Marik, T., Cuntz, M., Schmidt, M., Worthy, D.E., 1999. Verification of German methane emission inventories and their recent changes based on atmospheric observations. J. Geophys. Res. 104, 3447–3456. https://doi.org/10.1029/1998JD100064.

Liptay, K., Chanton, J., Czepiel, P., Mosher, B., 1998. Use of stable isotopes to determine methane oxidation in landfill cover soils. J. Geophys. Res. 1 (3), 8243–8250.

Lowry, D., Fisher, R.E., France, J.L., Coleman, M., Lanoisellé, M., Zazzeri, G., Nisbet, E. G., Shaw, J.T., Allen, G., Pitt, J., Ward, R.S., 2020. Environmental baseline monitoring for shale gas development in the UK: identification and geochemical characterisation of local source emissions of methane to atmosphere. Sci. Total Environ. 708, 134600. https://doi.org/10.1016/j.scitotenv.2019.134600.

Lowry, D., Holmes, C.W., Rata, N.D., O'Brien, P., Nisbet, E.G., 2001. London methane emissions: use of diurnal changes in concentration and δ ^{13}C to identify urban sources and verify inventories. J. Geophys. Res.: Atmosphere 106, 7427–7448. https://doi.org/10.1029/2000JD900601.

Miller, J.B., Tans, P.P., 2003. Calculating isotopic fractionation from atmospheric measurements at various scales. Tellus Ser. B Chem. Phys. Meteorol. 55B, 207–214. https://doi.org/10.1034/j.1600-0889.2003.00020.x.

Neelamani, S., Alawadhi, L., Alragum, A., alsudairawi, M., 2007. Extreme wind speed from different direction in Kuwait. Wind Eng. 31, 139–148. https://doi.org/10.1260/030952407781998846.

Nisbet, E.G., Manning, M.R., Dlugokencky, E.J., Fisher, R.E., Lowry, D., Michel, S.E., Lund Myhre, C., Platt, S.M., Allen, G., Bousquet, P., Brownlow, R., Cain, M., France, J.L., Hermansen, O., Hossaini, R., Jones, A.E., Levin, I., Manning, A.C., Myhre, G., Pyle, J.A., Vaughn, B., Warwick, N.J., White, J.W.C., 2019. Very strong atmospheric methane growth in the four years 2014 - 2017: implications for the Paris agreement. Global Biogeochem. Cycles 33, 318–342. https://doi.org/10.1029/2018GB006009.

Nisbet, E.G., Dlugokencky, E.J., Manning, M.R., Lowry, D., Fisher, R.E., France, J.L., Michel, S.E., Miller, J.B., White, J.W.C., Vaughn, B., Bousquet, P., Pyle, J.A., Warwick, N.J., Cain, M., Brownlow, R., Zazzeri, G., Lanoisellé, M., Manning, A.C., Gloor, E., Worthy, D.E.J., Brunke, E.G., Labuschagne, C., Wolff, E.W., Ganesan, A.L., 2016. Rising atmosphteric methane: 2007-2014 growth and isotopic shift. Global Biogeochem. Cycles 30, 1356–1370. https://doi.org/10.1002/2015GB005349. Received.

OPEC ASB Annual Statistical Bulletin, 2018. Annual report, 53rd edition. Available at: https://asb.opec.org/.

Paris, J.-D., Riandet, A., Bourtsoukidis, E., Delmotte, M., Berchet, A., Williams, J., Ernle, L., Tadic, I., Harder, H., Lelieveld, J., 2021. Shipborne measurements of methane and carbon dioxide in the Middle East and Mediterranean areas and contribution from oil and gas emissions. Atmos. Chem. Phys. 21, 12443–12462. https://doi.org/10.5194/acp-21-12443-2021.

Pataki, D.E., Ehleringer, J.R., Flanagan, L.B., Yakir, D., Bowling, D.R., Still, C.J., Buchmann, N., Kaplan, J.O., Berry, J.A., 2003. The aapplication and interpretation of keeling plots in terrestrial carbon cycle research. Global Biogeochem. Cycles 17 (Issue 1). https://doi.org/10.1029/2001GB001850.

Phillips, N.G., Ackley, R., Crosson, E.R., Downd, A., Hutyra, L.R., Brondfield, M., Karr, J. D., Zhao, K., Jackson, R.P., 2013. Mapping urban pipeline leaks: methane leaks across Boston. Environ. Pollut. 173, 1–4. https://doi.org/10.1016/j.envpol.2012.11.003.

Picarro [Online]. Available at: http://www.picarro.com.

United Nations, 2020. Reducing Gas Flaring in Arab Countries, A Sustainable Development Necessity. https://www.unescwa.org/publications/reducing-gas-flaring-arab-countries.

Rella, C.W., Hoffnagle, J., He, Y., Tajima, S., 2015. Local- and regional-scale measurements of CH_4, $\delta^{13}CH_4$, and C_2H_6 in the Uintah basin using a mobile stable isotope analyzer. Atmospheric Meas. Tech. 8, 4539–4559. https://doi.org/10.5194/amt-8-4539-2015.

Saunois, M., Bousquet, P., Poulter, B., Peregon, A., Ciais, P., Canadell, J.G., Dlugokencky, E.J., Etiope, G., Bastviken, D., Houweling, S., Janssens-Maenhout, G., Tubiello, F.N., Castaldi, S., Jackson, R.B., Alexe, M., Arora, V.K., Beerling, D.J., Bergamaschi, P., Blake, D.R., Brailsford, G., Brovkin, V., Bruhwiler, L., Crevoisier, C., Crill, P., Covey, K., Curry, C., Frankenberg, C., Gedney, N., Höglund-Isaksson, L., Ishizawa, M., Ito, A., Joos, F., Kim, H.S., Kleinen, T., Krummel, P., Lamarque, J.F., Langenfelds, R., Locatelli, R., Machida, T., Maksyutov, S., McDonald, K.C., Marshall, J., Melton, J.R., Morino, I., Naik, V., O'Doherty, S., Parmentier, F.J.W., Patra, P.K., Peng, C., Peng, S., Peters, G.P., Pison, I., Prigent, C., Prinn, R., Ramonet, M., Riley, W.J., Saito, M., Santini, M., Schroeder, R., Simpson, I.J., Spahni, R., Steele, P., Takizawa, A., Thornton, B.F., Tian, H., Tohjima, Y., Viovy, N., Voulgarakis, A., Weele, M., Werf, G.R., Weiss, R., Wiedinmyer, C., Wilton, D.J., Wiltshire, A., Worthy, D., Wunch, D., Xu, X., Yoshida, Y., Zhang, B., Zhang, Z., Zhu, Q., 2016. The global methane budget 2000-2012. Earth Syst. Sci. Data 8, 697–751. https://doi.org/10.5194/essd-8-697-2016.

Saunois, M., Stavert, A.R., Poulter, B., Bousquet, P., Canadell, J.G., Jackson, R.B., Raymond, P.A., Dlugokencky, E.J., Houweling, S., Patra, P.K., Ciais, P., Arora, V.K., Bastviken, D., Bergamaschi, P., Blake, D.R., Brailsford, G., Bruhwiler, L., Caelson, K. M., Carrol, M., Castaldi, S., Chandra, N., Crevoisier, C., Crill, P.M., Covey, K., Curry, C.L., Etiope, G., Frankenberg, C., Gedney, N., Hegglin, M.I., Höglund-Isaksson, L., Hugelius, G., Ishizawa, M., Ito, A., Janssens-Maenhout, G., Jensen, K.M., Joos, F., Kleinen, T., Krummel, P.B., Langenfelds, R.L., Laruelle, G.G., Liu, L., Machida, T., Maksyutov, S., McDonald, K.C., McNorton, J., Miller, P.A., Melton, J.R., Morino, I., Müller, J., Mueguia-Flores, F., Naik, V., Niwa, Y., Noce, S., O'Doherty, S., Parker, R.J., Peng, C., Peng, S., Peters, G.P., Prigent, C., Prinn, R., Ramonet, M., Regnier, P., Riley, W.J., Rosentreter, J.A., Segers, A., Simpson, I.J., Shi, H., Smith, S. J., Steele, L.P., Thornton, B.F., Tian, H., Tohjima, Y., Tubiello, F.N., Tsuruta, A., Viovy, N., Voulgarakis, A., Weber, T., Weele, M.V., Werf, G.R., Weiss, R.F., Worthy, D., Wunch, D., Yin, Yi, Yoshida, Y., Zhang, W., Zhang, Z., Zhao, Y., Zheng, B., Zhu, Q., Zhu, Q., Zhuang, Q., 2020. The global methane buget 2000-2017. Earth Syst. Sci. Data 12, 1561–1623. https://doi.org/10.5194/essd-12-1561-2020.

Schwietzke, S., Sherwood, O.A., Bruhwiler, L.M.P., Miller, J.B., Etiope, G., Dlugokencky, E.J., Michel, S.E., Arling, V.A., Vaughn, B.H., White, J.W.C., Tans, P. P., 2016. Upward revision of global fossil fuel methane emissions based on isotope database. Nature 538, 88–91. https://doi.org/10.1038/nature19797.

Sturm, P., Leuenberger, M., Schmidt, M., 2005. Atmospheric O_2, CO_2 and $\delta^{13}C$ observations from the remote sites jungfraujoch, Switzerland, and puy de Dôme, France. Geophys. Res. Lett. 32, 1–4. https://doi.org/10.1029/2005GL023304.

Townsend-Small, A., Tyler, S.C., Pataki, D.E., Xu, X., Christensen, L.E., 2012. Isotopic measurements of atmospheric methane in Los Angeles, California, USA: influence of 'fugitive' fossil fuel emissions. J. Geophys. Res, Atmos. 117, 1–11. https://doi.org/10.1029/2011JD016826.

Wang, P., Zhou, W., Niu, Z., Cheng, P., Wu, S., Xiong, X., Lu, X., Du, H., 2018. Emission characteristics of atmospheric carbon dioxide in Xi'an, China based on the measurements of CO_2 concentration, $\delta^{14}C$ and $\delta^{13}C$. Sci. Total Environ. 619–620, 1163–1169. https://doi.org/10.1016/j.scitotenv.2017.11.125.

World Meteorological Organisation, 2020. (WMO) greenhouse gas bulletin. No. 16.23 Novembet2020 [Online]. Available at: https://public.wmo.int/en/resources/library/wmo-greenhouse-gas-bulletin. (Accessed 18 April 2021).

World Meteorological Organization (WMO), 2018. Kuwait weather information service. available at: http://worldweather.wmo.int/en/city.html?cityId=217. .

Worthy, D.E.J., Levin, I., Trivett, N.B.A., Kuhlmann, A.J., Hopper, J.F., Ernst, M.K., 1998. Seven years of continuous methane observations at a remote boreal site in Ontario, Canada. J. Geophys. Res, Atmos. 103, 15995–16007. https://doi.org/10.1029/98JD00925.

Wuebbles, D.J., Hayhoe, K., 2002. Atmospheric methane and global change. Earth Sci. Rev. 57, 177–210.

Yamada, K., Yoshida, N., Nakagawa, F., Inoue, G., 2005. Source evaluation of atmospheric methane over western siberia using double stable isotopic signatures. Org. Geochem. 36, 717–726. https://doi.org/10.1016/j.orggeochem.2005.01.016.

Yassin, M.F., Almutairi, S.K., Alhemoud, A., 2018. Dust storms backward Trajectories' and source identification over Kuwait. Atmosphric Research 212, 158–171. https://doi.org/10.1016/j.atmosres.2018.05.020.

Zazzeri, G., Lowry, D., Fisher, R.E., France, J.L., Lanoisellé, M., Nisbet, E.G., 2015. Plume mapping and isotopic characterisation of anthropogenic methane sources. Atmos. Environ. 110, 151–162. https://doi.org/10.1016/j.atmosenv.2015.03.029.

Zazzeri, G., Lowry, D., Fisher, R.E., France, J.L., Lanoisellé, M., Grimmond, C.S.B., Nisbet, E.G., 2017. Evaluating methane inventories by isotopic analysis in the London region. Sci. Rep. 7, 1–13. https://doi.org/10.1038/s41598-017-04802-6.

Zhou, L.X., Worthy, D.E.J., Lang, P.M., Ernst, M.K., Zhang, X.C., Wen, Y.P., Li, J.L., 2004. Ten years of atmospheric methane observations at a high elevation site in western China. Atmos. Environ. 38, 7041–7054. https://doi.org/10.1016/j.atmosenv.2004.02.072.